Dynamics of a Probe Molecule Dissolved in Several Polymer Matrices with Different Side-Chain Structures: Determination of Correlation Length Relevant to Glass Transition

DATASET *in* MACROMOLECULES · MARCH 2013

Impact Factor: 5.8 · DOI: 10.1021/ma302567j

4 AUTHORS:

Shogo NOBUKAWA
Nagoya Institute of Technology
59 PUBLICATIONS **209** CITATIONS

SEE PROFILE

Osamu Urakawa
Osaka University
68 PUBLICATIONS **944** CITATIONS

SEE PROFILE

Toshiyuki Shikata
Tokyo University of Agriculture and Technology
115 PUBLICATIONS **2,686** CITATIONS

SEE PROFILE

Tadashi Inoue
Osaka University
139 PUBLICATIONS **1,694** CITATIONS

SEE PROFILE

Macromolecules

Article

pubs.acs.org/Macromolecules

Dynamics of a Probe Molecule Dissolved in Several Polymer Matrices with Different Side-Chain Structures: Determination of Correlation Length Relevant to Glass Transition

Shogo Nobukawa,*[,†,‡] Osamu Urakawa,*[,†] Toshiyuki Shikata,[†,§] and Tadashi Inoue[†]

[†]Department of Macromolecular Science, Graduate School of Science, Osaka University, 1-1 Machikaneyama-cho, Toyonaka, Osaka 560-0043, Japan

[‡]School of Materials Science, Japan Advanced Institute of Science and Technology, Nomi, Ishikawa 923-1292, Japan

ABSTRACT: Dynamics of 4-pentyl-4′-cyanobiphenyl (5CB) dissolved in several polymers at concentrations of 3−7 wt % was examined by dielectric relaxation measurement. Glassy (segmental) mode of the matrix polymer was also investigated by viscoelastic measurements for the same samples. Polystyrene (PS), poly(4-methylstyrene) (P4MS), and poly(4-*tert*-butylstyrene) (PtBS) were used as host polymers, considering that they have the same backbone structure but different side-chain bulkiness. Two dielectric relaxation modes (slow and fast modes) of 5CB component appeared in all the mixtures, and the relative intensity of the fast mode increased in the order of PS < P4MS < PtBS, corresponding to the order of the side-chain bulkiness and main-chain stiffness. The effects of such chemical structure differences on the two relaxation modes, particularly their temperature dependence, were examined in detail. Comparison of relaxation times for the fast mode and the segmental dynamics of the matrix polymer suggests that the fast mode was attributed to the restricted orientational fluctuation, which includes precession motion around the long axis, of 5CB molecule in a confined space formed by slow polymer chains. The dielectric intensity of the fast mode increased with increasing side-chain bulkiness of polymers. This means that the larger side chain decreases the spatial restriction for the movement of guest 5CB molecules in the glassy state. The slow mode was attributed to the rotational motion of 5CB molecule nearly cooperative with the segmental motion of matrix polymer. The relaxation times of dielectric slow mode and viscoelastic glass mode were compared. Temperature dependence of the slow mode was slightly different from that of the segmental motion of polymer corresponding to the glass mode. From the difference between these relaxation times, the correlation length relevant to the glass mode was determined as functions of temperature for the three polymers.

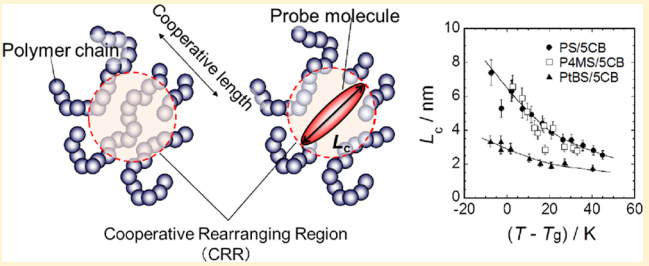

1. INTRODUCTION

The glass transition of materials including polymers, low-mass molecules (LMs), miscible polymer blends, and polymer/LM mixtures has been widely studied for years.[1−19] By cooling a material close to the glass transition temperature, T_g, the glassy relaxation process (sometimes referred to as α-relaxation or segmental relaxation) is observed by viscoelastic (and also dielectric) measurements. Temperature dependence of its relaxation time can be described with the Williams−Landel−Ferry (WLF) equation.[5] In the case of polymers, the most "relevant" motion to this relaxation mode is the micro-Brownian motion of chain segment. In contrast, in neat LM systems the rotational motion of LMs is relevant to this relaxation.[20]

Some polymer blends and polymer/LM mixtures, even in the miscible state, are known to exhibit very broad glass transition revealed by differential scanning calorimetry (DSC) measurement.[15,16] It has also been clarified that the component dynamics in such mixtures has different temperature dependence. This means that each component has its own effective glass transition temperature, T_g^{eff}, if temperature dependence of the component relaxation time is described by the WLF equation based on each T_g^{eff}.[13,21−23] Such phenomena are generally called "dynamic heterogeneity".[24,25]

Adachi et al. studied the dynamic heterogeneity of polystyrene (PS)/toluene (Tol) mixtures through NMR, dielectric relaxation, and heat capacity measurements.[21,26,27] In this system, the rotational motion of Tol molecule decoupled from the segmental motion of PS near the nominal (average) T_g. Furthermore, temperature dependence of the heat capacity showed two step glass transitions; these two transitions occurred approximately at each T_g^{eff} of the two components. These experimental results show that PS/Tol system is dynamically heterogeneous. On the other hand, trace amounts of fluorescence dyes dissolved in polymer matrices have been intensively used to probe the matrix polymer dynamics near the glass transition by optical methods.[7,12,28] In these studies, the probe motion was anticipated to be

Received: December 13, 2012
Revised: March 10, 2013
Published: March 15, 2013

cooperative with the polymer motion. However, dynamic heterogeneity of the PS/Tol system indicates that at least Tol molecule cannot be used as a probe molecule to extract the PS dynamics. Then, a fundamental question arises: what kind of molecules can be used as a probe to investigate the matrix polymer dynamics?

We have been focusing on the molecular size of LMs, which will be the key factor, whether or not the LM dynamics couple with the matrix polymer dynamics. For the larger size of LMs, the coupling will be stronger. By using LMs with much higher polarity compared to the matrix polymer component, only the dielectric relaxation of LMs could be observed. By such a method, Urakawa et al.[13,22] and van den Berg et al.[29] specified the critical size of LMs to be between 0.65 and 1.1 nm in the PS matrix, at which LM motion and segmental motion of PS couple each other; i.e., there is a crossover for both component dynamics from heterogeneous to homogeneous. The estimated critical LM size was comparable with the length of Kuhn segment of PS (1.79 nm).[13,22] According to Inoue[30] and Matsumiya et al.,[31] the size of the dynamic segment corresponding to the (Rouse) beads−spring units for PS is similar to that of the Kuhn segment. Therefore, the critical LM size estimated in their studies seems reasonable. It was also found that the component dynamics in a dynamically homogeneous PS/4-pentyl-4′-cyanobiphenyl (5CB) mixtures, i.e., rotational motion of 5CB, whose long axis is longer than the critical size, and global motion of PS (terminal relaxation), had the same temperature dependence at $T > T_g + 20$ K.[32] This result supported Urakawa's conclusion. However, it is not clarified yet whether or not the same T dependence holds in the vicinity of T_g and how much difference there is in the absolute values of the relaxation time between the rotational mode of 5CB and the segmental mode of polymers.

Viscoelastic relaxation spectra for polymeric systems are known to be separable into two modes reflecting the two different molecular motions: the terminal mode (including rubbery region) originating in the orientation relaxation of whole polymer chains and the glass mode due to more local motion. The terminal mode can be described by several course-grained models such as tube model,[33] beads−spring model,[34] and so on. The motional unit to be considered for the chain dynamics from the terminal to the rubbery region is so-called "Rouse segment", whose size will not change by changing the temperature. In contrast, the glass mode has the characteristic length scale which will be determined by both intra- and intermolecular interactions and is often denoted as just "glass segment" or "cooperative rearranging region (CRR)". Here, "glass segment" is a dynamical unit in a single chain determined by both the intra- and intermolecular interactions, while "CRR" is the dynamical unit including neighbor molecules with which cooperative motion takes place.[17−19] Therefore, the notions of "segment" and "CRR" are not necessarily the same even though they will have the similar length scales. Those sizes are believed to be dependent on temperature in the vicinity of T_g.[35] In this paper we compare the rotational motion of 5CB in dynamically homogeneous 5CB/polymer mixtures with the viscoelastic glass mode as functions of temperature and the relevant length scale of the glass mode is determined from the length (long axis) of the rodlike LM molecule whose rotational relaxation time coincides with the segmental relaxation time of polymer components.[13,32]

Concerning the LM motion in polymer/LM mixtures, one important finding in our previous studies[32] is the existence of two separated relaxation modes (slow and fast modes) both related to the LM motion. From the composition dependence of the fraction for the two modes, we concluded that the rotational dynamics of a 5CB molecule took place in two steps. The temperature dependence of relaxation time for the slow mode was similar to that for the global chain dynamics, suggesting that the slow mode is governed by the fundamental dynamical process of the coarse-grained polymer chain. On the other hand, the fast mode was not coupled to the chain dynamics since it showed weaker temperature dependence than the polymer chain motion. The LM concentrations of 5−20 wt % (utilized in the previous study) are in the region where the LM molecules are nearly isolated since the distance between LMs (1.6−2.5 nm) is longer than the molecular size (1.3 nm in the long axis). Therefore, the LM molecules are almost surrounded by polymers whose dynamics is slower than the LM component. From this reason, the confinement effect by the slow polymer matrix will make the LM dynamics be localized. The fast mode was attributed to the restricted motion (or wobbling motion) of LMs in a confined space which we call "cage" formed by less mobile polymer chains. Furthermore, we think that the fast mode includes the precession motion of rodlike LMs about the long axis because it has lower energy barrier than the fully rotational motion. This was also reported by van der Berg et al.[29]

When a polymer has larger pendant groups, the intermolecular distance between the polymer backbones becomes farther. In this case, the cage restriction will be weakened, probably resulting in the enhancement of the fast mode motion of LMs. In this study, in order to evaluate the effect of the side-chain bulkiness, polystyrene (PS) and its derivatives, poly(4-methylstyrene) (P4MS) and poly(4-*tert*-butylstyrene) (PtBS), were used as matrix polymers. 5CB was chosen as a guest molecule of these three polymers. Dielectric and viscoelastic measurements can probe the 5CB and polymer dynamics, respectively, because of the following reasons; 5CB is dielectrically more active due its larger dipole moment than PS even though the concentration is low (3−7 wt %), and PS is mechanically more responsive due to its high concentration and larger molecular sizes.

In our previous study only PS was examined as polymer matrix. By varying polymer structures, the generality of the dynamical features observed in PS/LM systems will be confirmed. The followings are the purposes of this study to be clarified: (1) examination of the relationship between the slow mode relaxation time of 5CB, τ_{5CB}, and segmental relaxation time of PS, τ_{seg}, (2) determination of the relevant length scale to the glass mode relaxation for the three polymers from the values of τ_{5CB} and τ_{seg}, and (3) examination of the effect of the side chain bulkiness on the fast mode relaxation of LMs.

2. EXPERIMENTAL SECTION

2.1. Materials. Polystyrene (PS), poly(4-methylstyrene) (P4MS), and poly(4-*tert*-butylstyrene) (PtBS) were synthesized by a living anionic polymerization of three monomers (styrene, 4-methylstyrene, and 4-*tert*-butylstyrene) with *sec*-butyllithium as an initiator in benzene solution. The weight-average molecular weight, M_w, and molecular weight distribution, M_w/M_n, where M_n is a number-average molecular weight, were determined by gel-permeation chromatography (GPC), and the results are shown in Table 1. 4-Pentyl-4′-cyanobiphenyl (5CB) was purchased from Wako Pure Chemical Industries, Ltd., and used as received. The chemical structures of all samples are shown in Figure 1.

dx.doi.org/10.1021/ma302567j | Macromolecules 2013, 46, 2206−2215

Table 1. Weight-Average Molecular Weight, M_w, Molecular Weight Distribution, M_w/M_n, Glass Transition Temperature, T_g, the Kuhn Segment Length, l_K, and Dielectric Relaxation Intensity, $\Delta\varepsilon$, for PS, P4MS, and PtBS

	$M_w/10^4$	M_w/M_n	T_g (K)	l_K[a] (nm)	$\Delta\varepsilon_{theo}$[b] (373 K)
PS	1.59	1.05	373	1.79	0.038
P4MS	11.1	1.08	387	2.17	0.0074
PtBS	4.51	1.06	419	2.30	0.0064

[a]Determined from literature data[37,38] for characteristic ratio C_∞ or mean-square radius $\langle S^2\rangle$. [b]Estimated by the Onsager equation with dipole moment values calculated by WinMopac software (Fujitsu, Japan).

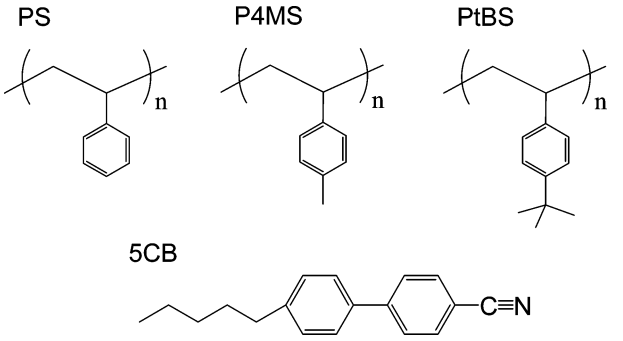

Figure 1. Chemical structures of polystyrene (PS), poly(4-methylstyrene) (P4MS), poly(4-*tert*-butylstyrene) (PtBS), and 4-pentyl-4′-cyanobiphenyl (5CB).

To prepare blend samples, polymer and 5CB at a weight ratio of 95/5 were dissolved into benzene, and then the solvent (benzene) was removed by the freeze-dry method. To remove any air bubbles and solvents remained inside the sample, all samples for dielectric and viscoelastic measurements were annealed above T_g under vacuum for half a day. Since 5CB slightly vaporized under vacuum, the blend compositions could not be precisely determined by weighting. Therefore, the weight fraction of 5CB, W_{5CB}, was determined by NMR measurement using EXcalibur-270 (JEOL Ltd., Tokyo, Japan) or Mercury-300 (Varian, Palo Alto, CA) for deuterated chloroform solutions in which the small portion of the blend film was dissolved. The W_{5CB} values determined by NMR are shown in Table 2. The compositions were checked before and after the dielectric and viscoelastic measurements and confirmed that the values were almost unchanged.

2.2. Measurements. A dielectric relaxation (DR) measurement was performed using three instruments: LCR meter (4284A, Hewlett-Packard), fast Fourier transform (FFT) analyzer (VC-2440, Hitachi, Japan), and impedance analyzer (β analyzer, Novocontrol Technologies GmbH & Co. KG, Germany). Temperature and frequency ranges were 300−430 K and 1 mHz−3 MHz, respectively. To obtain dielectric data as functions of temperature, dielectric permittivity was measured at frequencies scanned from 12 Hz to 200 kHz by an LCR meter (1693, Quad Tech Inc.) under gradual increase of temperatures from 100 to 450 K with a heating rate of 0.3 K min^{-1}.

A dynamic viscoelastic relaxation measurement was conducted using a stress rheometer (Physica MCR 301, Anton Paar GmbH, Austria) equipped with 4 mm parallel plate for the same samples for which the DR measurements were made. The temperature and frequency ranges were 338−453 K and 0.1−100 s^{-1}, respectively.

A differential scanning calorimetry (DSC) measurement was performed to determine the glass transition temperature, T_g, for each mixture from the midpoint of the jump in the heat flow around the glass transition by using a differential calorimeter (DSC 6220, EXSTAR-6000, Seiko Instruments Inc., Japan). After the viscoelastic measurements, T_g values were checked again to confirm that the composition of mixtures did not change. The determined T_g values for pure polymers and mixtures are shown in Tables 1 and 2, respectively.

3. RESULTS AND DISCUSSION

3.1. Dielectric Relaxation Behavior of 5CB Dissolved in Three Polymers. To examine the side-chain effect on the LM dynamics in polymer/LM mixtures, dielectric relaxation behaviors of 5CB dissolved in PS, P4MS, and PtBS matrices are compared. Urakawa et al.[13] indicated that the LM motion became cooperative with the dielectric α dynamics of PS when the LM size is comparable to or larger than the Kuhn length, l_K, of PS. Since the l_K value is known to be almost the same with the Rouse segment size,[36−38] we estimated the corresponding lengths for PS, P4MS, and PtBS to be 1.79, 2.17, and 2.30 nm, respectively (listed in Table 1), from the reported molecular weight of the Rouse segment,[39] M_{seg}, and the mean-square end-to-end distance divided by the molecular weight of a repeating unit,[40] $\langle R^2\rangle_0/M$. Note that this length increases with the size of the pendant group of polymers.

Complex dielectric permittivity, ε^* (= $\varepsilon' - i\varepsilon''$), was measured as a function of temperature, T, and angular frequency, ω, for PS/5CB, P4MS/5CB, and PtBS/5CB mixtures. Here, ε' and ε'' are dielectric permittivity and loss, respectively. Figure 2 shows the $T - T_g$ dependence of

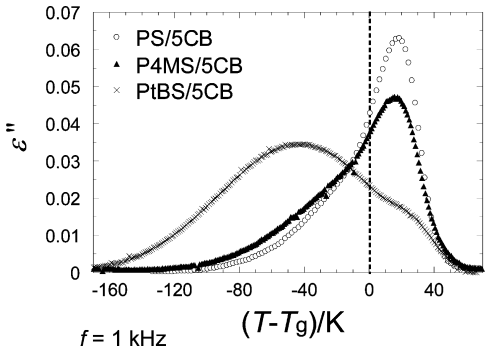

Figure 2. Temperature dependence of dielectric loss, ε'', for PS/5CB, P4MS/5CB, and PtBS/5CB blends at 1 kHz. The temperature axis is normalized by each glass transition temperature, T_g.

dielectric loss measured at $\omega = 6.3 \times 10^3$ s^{-1} for three mixtures containing a small amount of 5CB. Although the content of

Table 2. Weight Fraction of 5CB and T_g for Various Polymer/5CB Mixtures; Dielectric Intensities, $\Delta\varepsilon_{slow}$, $\Delta\varepsilon_{fast}$, and $\Delta\varepsilon_{total}$ (= $\Delta\varepsilon_{slow} + \Delta\varepsilon_{fast}$), Which Were Obtained at T_g + 20 K by Fitting the Data with Eq 2; Apparent Activation Energies for the Fast Mode of 5CB, $E_{a,h}$ and $E_{a,l}$

mixture	W_{5CB}	T_g (K)	$\Delta\varepsilon_{theo}$ ($\Delta\varepsilon_{theo,5CB}$)	$\Delta\varepsilon_{slow}$	$\Delta\varepsilon_{fast}$	$\Delta\varepsilon_{total}$	$E_{a,l}$ (kJ mol^{-1})	$E_{a,h}$ (kJ mol^{-1})
PS	0.077	348	0.85 (0.81)	0.36	0.51	0.87	155 ± 10	205 ± 10
P4MS	0.044	373	0.42 (0.42)	0.09	0.34	0.44	85 ± 10	210 ± 20
PtBS	0.048	389	0.46 (0.46)	0.05	0.45	0.50	80 ± 10	185 ± 20

dx.doi.org/10.1021/ma302567j | *Macromolecules* 2013, 46, 2206−2215

5CB in PS (7.7 wt %) was higher than those in P4MS and PtBS (4.4 and 4.8 wt %, respectively), this difference does not affect the conclusion led by this study as will be mentioned later. Two relaxation processes appear below and above the T_g. In our previous study,[25] the major dispersion observed in PS/5CB above T_g was assigned to the rotational motion of 5CB, which was cooperative with the segmental motion of polymers (slow mode), and the low-temperature shoulder was ascribed to the orientation fluctuation of 5CB in a confined space by the glassy matrix (fast mode). The same assignment would be valid for the other two systems: P4MS/5CB and PtBS/5CB. The relative intensity of the slow mode becomes weaker with increasing the side chain size of the polymer (PS < P4MS < PtBS). Particularly, for the PtBS/5CB system, the fast mode becomes a major relaxation mode. This behavior indicates that side-chain structure strongly affects the dielectric relaxation behavior of the guest molecule.

Figure 3A shows the frequency dependence of ε' and ε'' measured at T_g + 2 K for the same samples shown in Figure 2. If the rotational motion of polar molecules is characterized by a single relaxation mode, the dielectric relaxation curve can be represented by the Debye function.[41] The ε'' curve of the Debye function is shown by the dashed curve in the Figure 3A for reference. The observed ε'' curves are quite broad compared with the Debye spectrum and have a clear bimodal shape except for PS/5CB, indicating that two kinds of molecular motion with very wide relaxation time distributions are involved in dielectric relaxation process. The top panel of this figure shows $\varepsilon' - \varepsilon_\infty$ as functions of ω, where ε_∞ is the limiting dielectric permittivity at high frequencies which can be determined by fitting the experimental data with eq 2 as will be mentioned later. The dielectric intensity, $\Delta\varepsilon$, is given by the difference between ε' at low frequencies ($\varepsilon'(\omega=0)$) and ε_∞ ($\Delta\varepsilon = \varepsilon'(0) - \varepsilon_\infty$). In the inset of this figure, the values of $\Delta\varepsilon$ are plotted against the weight fraction of 5CB, W_{5CB}. The plotted data include our previous results.[32] Dielectric intensity, $\Delta\varepsilon$, of the polar molecule in a continuous media is proportional to its volume fraction (~ weight fraction) if the polar molecules are uniformly dissolved without any orientation correlation for the electric dipoles. The linear relationship between $\Delta\varepsilon$ and W_{5CB} is observed in the range of weight fraction (~0.2), meaning that the observed broad and bimodal dielectric relaxation can be attributed to the response of only 5CB molecules. In other words, the dielectric relaxation of polymer component is negligible in the observed dielectric response.

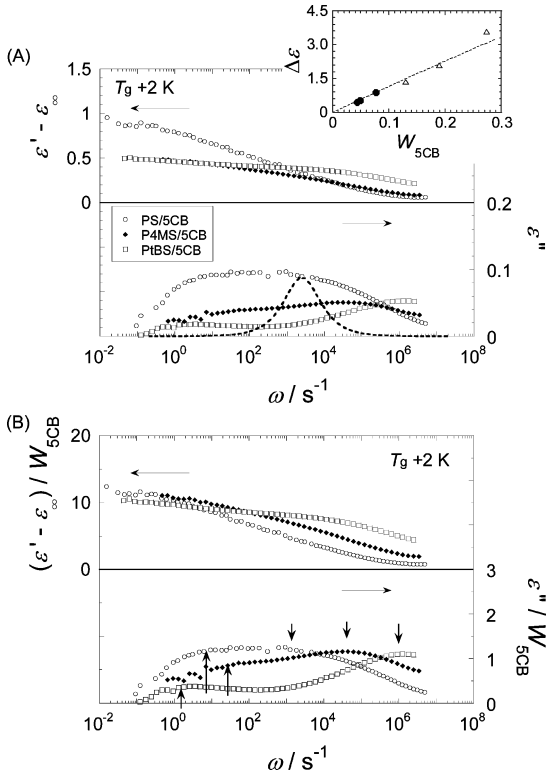

Figure 3. (A) Angular frequency, ω, dependences of dielectric permittivity and loss, ε' and ε'', for PS/5CB, P4MS/5CB, and PtBS/5CB mixtures at T_g + 2 K. The vertical axis on the left side indicates the difference between the ε' and the limiting permittivity at high frequency, ε_∞. The dashed line represents a single Debye function. The inset shows the relationship between $\Delta\varepsilon$ and W_{5CB} from the experimental data (closed circle) including our previous results (opened triangle) already reported.[32] (B) Frequency dependence of dielectric relaxation data divided by each weight fraction of 5CB, W_{5CB}, for mixtures. The arrows indicate the maximum frequencies for slow and fast relaxations which were determined by fitting with the Cole–Cole functions in eq 2.

In order to further check the validity of the above-mentioned discussion, the $\Delta\varepsilon$ value was calculated from the electric dipole moment, μ, based on the Kirkwood formula[42] which is the extension of the Onsager theory.[43]

$$\Delta\varepsilon = \varepsilon(0) - \varepsilon_\infty = g\frac{\rho\phi N_A}{M}\frac{\mu^2}{9\varepsilon_0 k_B T}\frac{(2+\varepsilon_\infty)^2}{2+\varepsilon_\infty/\varepsilon(0)} \quad (1)$$

Here, T is the absolute temperature, k_B is the Boltzmann constant, ε_0 is the dielectric constant (or the vacuum permittivity), N_A is Avogadro's number, and ρ is the density. M and ϕ are the molecular weight and the volume fraction of the polar molecule in mixture, respectively. The Kirkwood factor, g, represents the magnitude of the orientation correlation for the dipole vectors of polar molecules. Here we assume g = 1, since the concentration of 5CB is small enough. From the μ value of 5CB (4.4 D, 1 D = 3.33564 × 10^{-30} C m) and those of the monomer unit for PS (0.21 D), P4MS (0.09 D), and PtBS (0.11 D), which were estimated by WinMopac software (Fujitsu, Japan), dielectric intensities of all the components were calculated and are shown in the column of $\Delta\varepsilon_{theo}$ of Tables 1 and 2. In this calculation, the density values of 1.05, 1.02, and 0.95 g cm^{-3} for PS, P4MS, and PtBS, respectively, were used, and as for the ε_∞ values, those of the corresponding neat polymers (2.51, 2.53, and 2.53, respectively) were used as an approximation considering the low concentration of 5CB. A comparison of $\Delta\varepsilon$ values between polymers and 5CB, which are tabulated in Tables 1 and 2, indicates that the contributions of PS, P4MS, and PtBS components to the dielectric intensity are negligibly small. In addition, due to the similarity of the refractive index and density, eq 1 gives the linear relation, $\Delta\varepsilon \propto \phi_{5CB}$ ($\propto W_{5CB}$), in accord with the result shown in Figure 3A. Therefore, it can be concluded that the observed dielectric responses can be attributed only to the molecular motion of the 5CB component.

For the quantitative comparison, both $\varepsilon' - \varepsilon_\infty$ (= $\Delta\varepsilon'$) and ε'' data were divided by W_{5CB} and are shown in Figure 3B. The $\Delta\varepsilon'/W_{5CB}$ value of three samples at the limiting low frequency agrees with each other in experimental error, indicating that the sum of the relaxation intensities of two relaxation modes is

dx.doi.org/10.1021/ma302567j | Macromolecules 2013, 46, 2206–2215

constant. This means that the rotational motion of 5CB takes place in two steps: partial rotational relaxation of 5CB via wobbling motion and/or spinning motion about the long axis at high frequency (fast mode) and full rotational relaxation at low frequency (slow mode). In Figure 3B, the maximum frequencies for the fast and slow modes are indicated by the arrows which were determined by fitting the relaxation curves with eq 2 being discussed later. The difference in maximum frequencies of the slow mode for three samples are within 1 decade at T_g +2 K, while that of the fast mode is larger (more than 3 decades difference) and the peak frequencies shift higher side with increasing the side-chain size and the Kuhn length (PS < P4MS < PtBS). Furthermore, the relative intensity of the slow mode decreases in the order of PS < P4MS < PtBS and vice versa for the fast mode. Concerning the large difference in the fast mode relaxation times for three polymers, it depends on temperature; the difference becomes larger with decreasing temperature because of the different activation energies as will be shown in Figure 11. Additionally, the bimodal dielectric spectra for the three systems became wider with decreasing temperature, suggesting that the two modes have different temperature dependence.

These changes in the shape of dielectric spectra with polymer structures could be thought to be due to the difference in the molecular packing around 5CB molecules in the mixtures. In the case of PtBS, the larger side chain and longer Kuhn length will allow 5CB molecules to rotate with wider angle before the polymer backbone (segment) motion starts, and thus the amplitude of the local fluctuation motion (fast mode) would be larger. On the other hand, in the case of PS, the average distance between polymer chain backbone will be shorter compared with the case of PtBS and P4MS due to the smaller side group and higher backbone flexibility; the local wiggling motion of 5CB has small amplitudes. Thus, the fast mode strongly reflects the difference in local environment surrounding the guest 5CB molecule which will be determined by both the chain stiffness and the side-chain bulkiness.

3.2. Dielectric Relaxation Intensity and Time of 5CB in Mixtures. Since all the obtained dielectric spectra are broad and bimodal, it is difficult to analyze them with a single Debye function.[41] For glass mode spectra of polymers, the Havliriak–Negami (H–N)[44] and Cole–Cole (C–C)[45] functions are generally used. As described in our previous paper,[32] although the H–N function can reproduce an asymmetric relaxation spectrum, it has larger number of parameters than the C–C function and thus gives some ambiguity in determining the fitting parameters: different combinations of the parameter sets are sometimes possible to fit the same dielectric spectra. In order to avoid this problem, we use the sum of two Cole–Cole type functions given by eq 2 to fit the data. We think this equation is enough to separate the dielectric spectra into two modes and to determine the average relaxation time and the relaxation strength of each mode.

$$\varepsilon^*(\omega) = \varepsilon_\infty + \sum_{j=\mathrm{slow,fast}} \frac{\Delta\varepsilon_j}{1 + (i\omega\tau_j)^{\alpha_j}} \qquad (2)$$

Here, $\Delta\varepsilon_j$, τ_j, and α_j are respectively relaxation intensity, relaxation time, and symmetric broadening parameter for j mode. In the case of the Debye function, α_j becomes unity. All the experimental data were successfully fitted by eq 2, and the used parameters, τ_j and $\Delta\varepsilon_j$, for the slow and fast modes almost coincided with those previously determined for PS/5CB.[32]

Figure 4 displays a typical result of the fit for the PtBS/5CB mixture at 390.7 K. The arrows show the relaxation frequencies

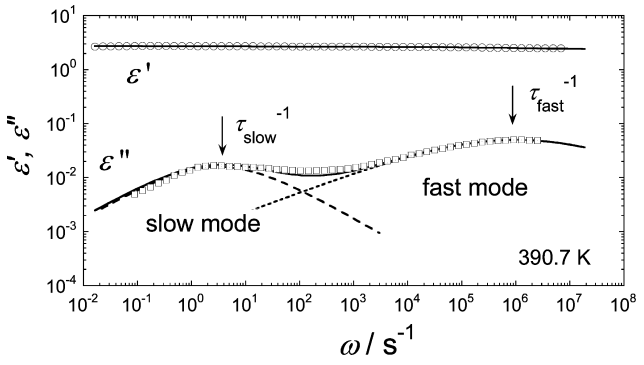

Figure 4. A typical dielectric spectrum of PtBS/5CB mixture at 390.7 K. The solid and dotted lines represent the best fit results by using eq 2.

corresponding to τ_{slow}^{-1} and τ_{fast}^{-1}. The α values for both modes were smaller than unity ($0.3 < \alpha < 0.7$), reflecting the broad relaxation time distribution. Figure 5 shows α_{slow} and α_{fast}

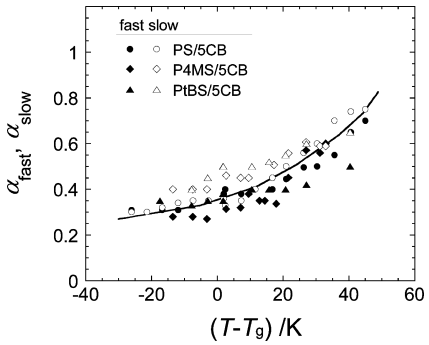

Figure 5. Temperature dependence of α_{fast} and α_{slow} for various mixtures. The temperature axis is normalized by each T_g.

values plotted against $T - T_g$. Both the values monotonically decrease with decreasing temperature, indicating the relaxation time distributions for both the slow and fast modes become broader at lower temperatures.

Although the broadness of the dielectric relaxation spectra changes with temperature, the relaxation times, τ_{slow} and τ_{fast}, reflect average rates of the two kinds of the 5CB motion in polymer matrices. In order to compare the dynamics of 5CB among three systems, PS/5CB, P4MS/5CB, and PtBS/5CB, all τ_{slow} and τ_{fast} data are shown as functions of $T - T_g$ in Figure 6. The τ_{slow} values increase with decreasing T and reach 1 s around $T = T_g$. This behavior is common for all the mixtures. In addition, Figure 6 shows that the temperature dependences of τ_{slow} for PS/5CB and P4MS/5CB are almost the same as functions of $T - T_g$ while that for PtBS/5CB is slightly different. This difference will reflect the nature of the glassy dynamics intrinsic to the matrix polymers as will be discussed later. Concerning the fast mode, we note that the τ_{fast} values are dependent on the polymer species, and their temperature dependence is different from that for τ_{slow}. These features will be discussed later. In the next section, the relationship between the 5CB motion and polymer dynamics will be examined in detail by comparing with the data of viscoelastic relaxation.

dx.doi.org/10.1021/ma302567j | Macromolecules 2013, 46, 2206–2215

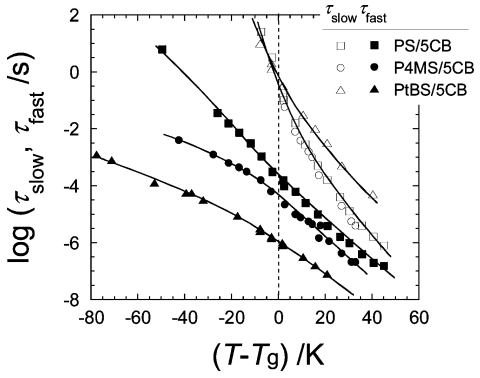

Figure 6. Temperature dependence of slow and fast relaxation times for 5CB, τ_{slow} and τ_{fast}, in PS/5CB, P4MS/5CB, and PtBS/5CB mixtures. The horizontal axis is normalized by each T_g.

3.3. Comparison of Dielectric and Viscoelastic Relaxation Behavior. Viscoelastic spectra of the mixtures from the glassy to the flow regions are shown in Figure 7, along

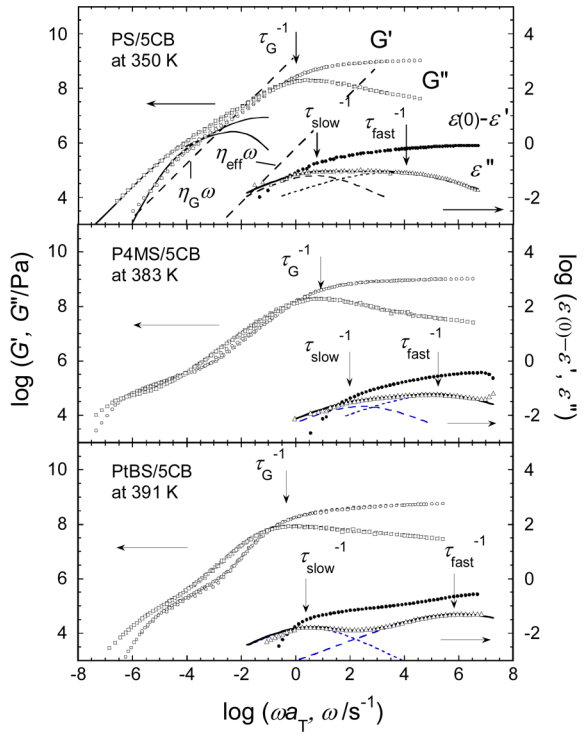

Figure 7. Comparison of composite curves for dielectric and viscoelastic spectra for PS/5CB, P4MS/5CB, and PtBS/5CB mixtures at the same reference temperature. Arrows indicate the maximum frequencies of the dielectric and viscoelastic losses for each data. The solid lines overlaid on the G^* curves represent the Rouse modes. The solid and dotted lines overlaid on ε'' curves are the fitted results with eq 2.

with the dielectric spectra obtained at the same reference temperature for comparison. The storage and loss moduli, G' and G'', respectively, over a wide range of frequencies were obtained by applying the method of reduced variables[4] to the viscoelastic data measured at several temperatures. Here a_T is the frequency shift factor. The viscoelastic spectra of PS/5CB and PtBS/5CB mixtures do not clearly show the rubbery plateau region because of the lower M_w value than the molecular weight between the entanglements, M_e (1.7×10^4 for PS, 3.7×10^4 for PtBS).[40] For those systems, the terminal region of the G^* can be well represented by the Rouse theory[34] as shown with the solid curves in Figure 6. On the other hand, the spectrum of P4MS/5CB exhibits the rubbery plateau region due to the entanglement effect because the M_w is higher than M_e, which is estimated as 1.9×10^4 by assuming the same number of repeating units with PS.

At high frequencies, G' reaches 10^9 Pa, which is the typical value for glassy materials. One maximum was observed in G'' for all the mixtures around the glass-to-rubber transition region. The inverse of the frequency at the loss modulus maximum can be regarded as the segmental relaxation time, τ_G, of polymer component, related to the glass transition.[46] Since we focus on the cooperativity between polymers and 5CB, the dielectric and viscoelastic relaxation times between components are compared. The arrows shown in Figure 7 indicate the maximum frequency corresponding to the inverse of the relaxation times, τ_G (segmental motion of polymers), τ_{slow}, and τ_{fast} (rotational and wobbling motion of 5CB) for each mixture. The segmental relaxation for the matrix polymer showed the broad distribution of the relaxation time and especially the relaxation function in the high-frequency region overlapped with the fast mode relaxation of 5CB. However, we think that the fast mode is more or less independent of the segmental motion of polymers because of the appearance of the "clear" peak in dielectric loss spectra, which cannot be explained as the motion of 5CB coupled with the high-frequency component of the segmental motion. Figure 7 shows that the τ_{slow} and τ_G look close, but τ_{slow} is about 10 times shorter than τ_G. This suggests that the slow mode of 5CB would reflect the smaller scale motion than the glass dynamics of polymers. In contrast, τ_{fast} locates at much shorter time region so that the fast mode should be attributed to more localized motion in a confined space by immobilized matrix polymers.

3.4. Slow Mode of 5CB and Glassy Relaxation Mode of Polymers. By using the method of reduced variables, temperature dependence of τ_G data over a wide temperature range were obtained and shown in Figure 8 along with τ_{slow} as functions of $T - T_g$. The dashed lines were fitted results of the data by using the WLF function.[5] Roland et al. indicated that the glass relaxation mode and terminal relaxation mode of amorphous polymers have different temperature dependence.[46] Inoue et al.[47] separated the viscoelastic spectra of homopolymer systems into rubbery (R) (= terminal) and glassy (G) modes and clearly showed that the R and G modes had different temperature dependence (different shift factors, a_T(R) and a_T(G)). However, the difference in the two shift factors, a_T(R) and a_T(G), is known to appear only in the vicinity of T_g. Although the determined a_T at high temperature (in the rubber ~ flow region) should be the R mode shift factor, the T dependence of a_T(R) and a_T(G) in this region will be the same, based on the data reported by Roland et al.[46] This means that the obtained nominal shift factors for G^* over all the temperature range approximately correspond to the a_T(G). Therefore, the temperature dependence of τ_G can be approximately determined from the nominal shift factors.

The figure shows that τ_G and τ_{slow} have slightly different temperature dependence and that there is a gap in their absolute values, suggesting that the slow mode of 5CB would not be completely coupled with the G mode of polymers. We tentatively attribute these features to the size difference between the 5CB molecule and the relevant length of the glass mode relaxation which might be dependent on temper-

dx.doi.org/10.1021/ma302567j | Macromolecules 2013, 46, 2206−2215

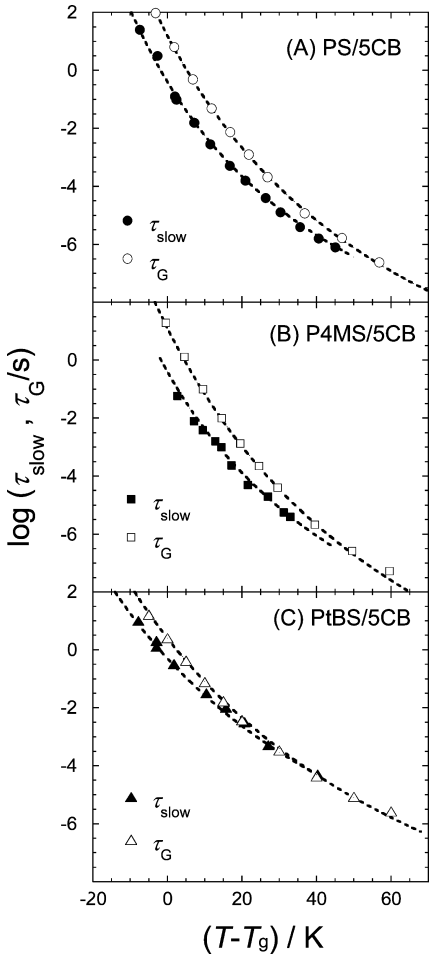

Figure 8. Temperature dependence of the relaxation times for viscoelastic G mode of polymers and dielectric slow mode of 5CB, τ_G and τ_{slow}, respectively. (A) PS/5CB, (B) P4MS/5CB, and (C) PtBS/5CB mixtures. The dotted lines are the best-fit results by using the WLF function,[5] $\tau = \tau_{ref} \exp[-c_1(T - T_{ref})/(c_2 + T - T_{ref})]$ with proper numbers of parameters for each mixture.

ature. Since τ_{slow} is about 2−100 times shorter than τ_G, the average size of the motional unit responsible for the glass mode relaxation (corresponding to the maximum of G'') will be larger than the size of 5CB, whose long axis is 1.3 nm. Moreover, τ_{slow} merges into the same line with τ_G at high temperature, indicating that the dynamical scale of the polymer segment becomes close to the 5CB size with increasing temperature. From the difference between τ_{slow} and τ_G, the relevant length scale for the G mode will be estimated in the next paragraph.

In several PS/LM mixtures,[32] the molecular size dependence of the rotational relaxation time for rodlike molecules was discussed previously based on the rotational diffusion theory.[48] We found that the dielectric relaxation time of several rodlike LMs, $\tau_{r,rod}^{DR}$, was proportional to the cube of the rod length, L, i.e., $\tau_{r,rod}^{DR} \propto L^3$. It is considered that the relaxation time is governed by the two factors: friction coefficient, $\zeta(T)$, and the length of the rodlike molecule.

$$\tau_{r,rod}^{DR} \sim \zeta(T)L^3 \tag{3}$$

Concerning the viscoelastic relaxation time of the glass mode, τ_G, the similar expression will be possible

$$\tau_G \sim \zeta(T)F(\xi) \tag{4}$$

Here, $F(\xi)$ is a structure factor determined by the relevant length of the glass mode relaxation, ξ. Colby proposed the scaling relation for τ_G as $\tau_G \sim \xi^z$ and suggested $z = 6$.[49] However, the friction factor is implicitly included in his equation, and thus it is not compatible with eq 4. Here, we assume that the functional form of $F(\xi)$ is the same with eq 3, i.e., $F(\xi) = \xi^3$. When the long axis of a rodlike molecule becomes comparable with the relevant length of the glassy mode, two experimentally observed relaxation times will become the same. We define this length of the rodlike molecule as critical length, L_c. From eqs 3 and 4, and the assumptions described above, we can determine L_c, by the following equation:

$$L_c = L_{5CB}\left(\frac{3\tau_G}{\tau_{slow}}\right)^{1/3} \tag{5}$$

Here τ_{slow} corresponds to $\tau_{r,rod}^{DR}$ in eq 3, and because of the difference in the rank between dielectric and viscoelastic relaxation times, the numerical factor 3 is incorporated. The L_c can be regarded as the relevant length of the glassy mode.

The L_c values in the three kinds of polymers, PS, P4MS, and PtBS, are estimated as functions of temperature and shown in Figure 9A. PS/5CB and P4MS/5CB mixtures have larger L_c, and their temperature dependence is stronger than the case of PtBS/5CB. This result will be related to the difference in

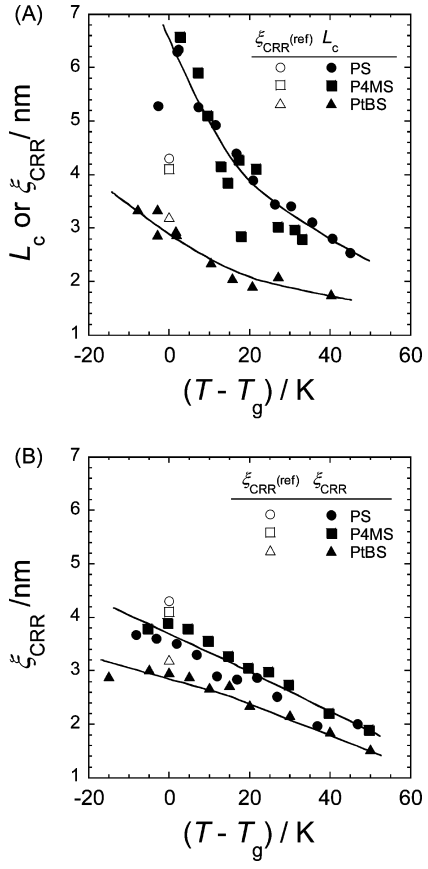

Figure 9. (A) Temperature dependence of the critical length, L_c, estimated by using eq 5. The size of CRR, ξ_{CRR} (ref), determined by Ellison et al.[12] is also shown. (B) Temperature dependence of ξ_{CRR} determined from the viscoelastic data by following Capaccioli et al.[18] The heat capacities for polymers were used from the data reported by Ellison et al.

dx.doi.org/10.1021/ma302567j | Macromolecules 2013, 46, 2206−2215

dynamic cooperativity and fragility of these three polymers as reported by Erwin and Colby.[50]

The idea of cooperative rearranging region (CRR), which was originally introduced by Adam and Gibbs,[2] is now one of the most important notions to explain thermodynamics of glass transition. The CRR is related to a subsystem, which can rearrange its configuration into another, independently of its environment upon a sufficient thermal fluctuation. Donth[17,51] theoretically related the volume of CRR to the change in heat capacity based on the Adam and Gibbs theory.[2] Ellison et al.[12] estimated the length scales of CRR, ξ_{CRR}, at T_g from the DSC data of PS, P4MS, and PtBS to be 4.3, 4.1, and 3.2 nm, respectively, using the Donth's theory, and the values are shown in Figure 9A. In a practical comparison of the L_c and ξ_{CRR} values, their reported ξ_{CRR} was corrected here by a factor of $(6/\pi)^{1/3}$ because they regarded the structure of CRR as cubic instead of sphere.

Capaccioli et al.[18] estimated the number of the repeating unit N_{CRR} from the results of thermal and dynamic relaxation measurements.

$$N_{CRR} = \frac{k_B}{\Delta C_p}\frac{N_A}{M_0}\left(\frac{\beta}{e}\right)^2\left(\frac{\mathrm{d}\ln\tau}{\mathrm{d}\ln T}\right)^2 \quad (6)$$

Here, ΔC_p is a specific heat capacity, M_0 is the molecular weight of a repeating unit, and β is the exponent in Kohlausch−Williams−Watts (KWW) function[52,53] $\phi(t)$, which can reproduce asymmetric relaxation spectrum for glassy polymers and is given by

$$\varphi(t) = \exp\left(-\frac{t}{\tau}\right)^{\beta} \quad (7)$$

From the τ_G data with using eq 6 and the relation of $N_{CRR} = (\pi\rho N_A/6M_0)\xi_{CRR}^3$, the size of CRR, ξ_{CRR}, for the three polymers were estimated. For this calculation, ΔC_p of bulk polymers[12] was used instead of polymer/5CB mixture's values because of the small content of 5CB. The results are also shown in Figure 9B. The length scale, ξ_{CRR}, estimated with the method by Capaccioli et al. is similar to that by Ellison et al., suggesting that the CRR size in the blend is almost the same with that in the bulk.

It can be seen that absolute values of L_c and ξ_{CRR} are different even though the trend of the sample dependence is the same: L_c is up to about twice larger than ξ_{CRR}. The estimation method of the ξ_{CRR} is based on the thermodynamic approach for the glass transition, which conflicts the kinetic nature of glass transition. In contrast, the L_c was estimated purely from dynamic data. Therefore, there will be a possibility that the ξ_{CRR} and the L_c have essential difference.

Interestingly, the order of the L_c values at T_g (6.1 ± 0.5, 6.6 ± 0.5, and 3.1 ± 0.3 nm in PS, P4MS, and PtBS mixtures) is not the same with that of the Kuhn segment length, l_K (1.79, 2.17, and 2.30 nm for PS, P4MS, and PtBS). The Kuhn length representing the polymer chain flexibility is determined by the potential barrier of the internal rotation along the C−C bond. Therefore, the difference in the length scales indicates that the critical length, L_c, of the guest molecule is associated with not only the intramolecular interaction but also the intermolecular cooperativity. On the basis of this idea, when polymers have long L_c and short l_K, e.g., in the case of PS and P4MS, the contribution of the intermolecular cooperativity will be higher. In contrast, when polymers have short L_c and long l_K, the intramolecular interaction will be dominant, e.g., in the case of PtBS.

Table 3. T_g, l_K, and the CRR Size, ξ_{CRR}, for PtBS, P4MS, and PS Taken from Literature Data;[12,38] Critical Length, L_c, of LM in the Mixtures Was Estimated from Eq 6

	T_g[a] (K)	l_K[a] (nm)	ξ_{CRR}[b] (nm)	L_c (nm)
PtBS	419	2.30	3.2	3.1
P4MS	387	2.17	4.1	6.6
PS	373	1.79	4.3	6.1

[a]Already shown in Table 1. [b]Data estimated by Ellison et al. based on the DSC measurements.[12]

The critical length, L_c, becomes close to l_K with increasing temperature, meaning that the intermolecular interaction becomes weaker with increasing temperature. Particularly, for PtBS at 40 °C higher than T_g, L_c is almost the same with l_K, and thus the intermolecular cooperativity will be negligible, and only the intramolecular interaction will dominate the segmental dynamics. In contrast, L_c's even at the highest temperatures ($T \sim T_g + 40$ K) for PS and P4MS are longer than l_K, indicating that the intermolecular interaction still affects the segmental dynamics at T_g + 40 K. Figure 9 shows that PS and P4MS systems exhibit stronger T-dependence than PtBS. Erwin and Colby[50] compared temperature dependences of the CRR size for some glass-forming liquids determined by 4D-NMR experiment and concluded that the temperature dependence of CRR size is stronger for materials with higher fragility index. Since PS and P4MS, whose L_c's have stronger temperature dependence, can be regarded to be more fragile than PtBS, it is concluded that a larger side chain decreases the fragility index.

3.5. Fast Mode of 5CB and Glass Transition. As mentioned in the Introduction, the fast mode of 5CB in mixtures was assigned to the orientational fluctuation of 5CB including the precession motion around the long axis, in the confined space (cage) surrounded by polymer chain backbones.[32] It is considered that both the cage size and the mobility inside the cage determine the fast mode relaxation. The cage structure will be determined by the molecular packing around a 5CB molecule including both the backbone and the side chains of polymers. As already mentioned in the previous section, the larger side chain and longer Kuhn length of polymers would cause the less confinement to the fluctuation motion of a 5CB molecule.

In order to discuss the detail of the fast mode relaxation, temperature dependence of the dielectric intensity, $\Delta\varepsilon_{fast}$, and relaxation time, τ_{fast}, are analyzed in this section. Figure 10 shows the plot of $\Delta\varepsilon_{fast}$ normalized by W_{5CB} vs T/T_g. The trend of increasing $\Delta\varepsilon_{fast}$ with temperature is observed. The dielectric intensity reflects the amplitude of the fluctuation motion of a 5CB molecule, and thus the increase of $\Delta\varepsilon_{fast}$ means that the confinement effect on the fluctuation motion weakens at higher temperature. This is understandable because the size of a cage which allows the fluctuation motion of a guest molecule will increase with temperature.[9,54]

Since the total dielectric intensity per one 5CB molecule is approximately constant in all three different mixtures, $\Delta\varepsilon_{fast}/W_{5CB}$ reflects the contribution of the restricted partial rotation to the full rotation of 5CB. As seen in Figure 10, the values of $\Delta\varepsilon_{fast}/W_{5CB}$ increases in the order of PS, P4MS, and PtBS, i.e., in the order of the Kuhn segment length or side chain bulkiness. Urakawa et al. reported that the fast mode intensity

dx.doi.org/10.1021/ma302567j | Macromolecules 2013, 46, 2206−2215

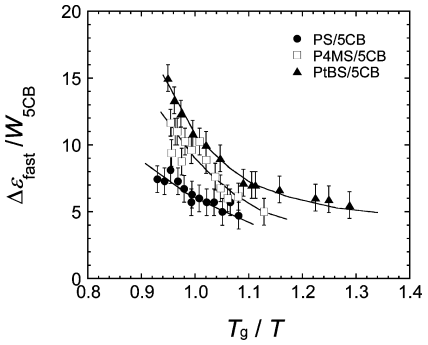

Figure 10. T_g/T dependence of the dielectric fast mode intensity normalized by the 5CB concentration for PS/5CB, P4MS/5CB, and PtBS/5CB mixtures.

increased with decreasing the LM size in the same PS matrix.[13,22] By taking into account all these results, it is concluded that the size ratios of the LM to the Kuhn segments and/or the side chain bulkiness of polymers determine the strength of the fast mode. We think both factors contribute to increase the cage size which will enhance the orientational fluctuation motion of LMs, resulting in the increase of $\Delta\varepsilon_{fast}$.

Figure 11 shows the plots of τ_{fast} against T_g/T. The time scale of fast mode appears to become shorter in the order of PS → P4MS → PtBS. Because it was found in the previous report[32] that τ_{fast} is independent of probe concentration in the plot against T_g/T, the difference in the time scale indicates that the restriction of 5CB by the matrix polymer will be weakened with increasing the side chain bulkiness. Additionally, the T_g/T dependence of τ_{fast} seems to consist of the two Arrhenius forms: Two linear lines with different slopes can be drawn in this plot. The temperatures, at which the slopes change, almost coincide with T_g for all the mixtures, indicating that the fast mode will be also affected by the glass transition. This behavior apparently resembles to the temperature dependence of specific volume or density for amorphous polymers and is also reported for the β relaxation of a probe molecules in the PS/probe systems by van den Berg et al.[29] and for the secondary relaxation in amorphous poly(methyl methacrylate) by Bergman et al.[55] Here, it is assumed that the T dependence of τ_{fast} can be expressed by the reciprocal sum of the two Arrhenius equations

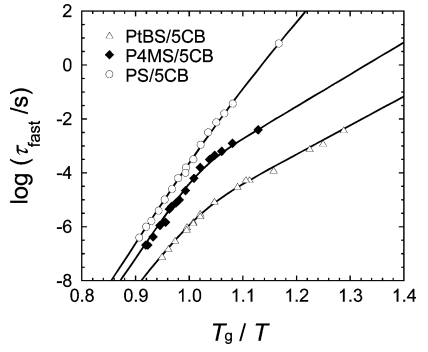

Figure 11. Plots of the fast mode relaxation time, τ_{fast}, against T_g/T for PS/5CB, P4MS/5CB, and PtBS/5CB mixtures. The solid lines represent the best fit results with the double Arrhenius function given by eq 7.

$$\tau_{fast} = \left[\frac{1}{\tau_h^{\infty}\exp(-E_{a,h}/RT)} + \frac{1}{\tau_l^{\infty}\exp(-E_{a,l}/RT)}\right]^{-1} \quad (8)$$

where E_a and τ^{∞} are the apparent activation energy and the limiting relaxation time at high temperatures, respectively. The subscripts "h" and "l" represent high and low temperature components. The solid lines shown in the figure represent the fitted result with eq 8. From these fitting, two activation energies, $E_{a,h}$ and $E_{a,l}$, were estimated and tabulated in Table 2. $E_{a,h}$ was similar among all the mixtures while $E_{a,l}$ decreased in the order of PS, P4MS, and PtBS. The confinement effect to the orientational fluctuation of 5CB becomes stronger with decreasing temperature, resulting in the increase of the relaxation time. However, the time necessary for the structural equilibration (toward the equilibrium molecular packing) becomes very long below T_g, and thus the deviation from the high-T Arrhenius equation will be due to the nonequilibrium structure. In this sense, the difference in the apparent activation energies below T_g will be related to the difference in the degree of equilibration among three systems.

4. CONCLUSION

In this paper, the dynamics of 4-pentyl-4′-cyanobiphenyl (5CB) dissolved in three polymers—polystyrene (PS), poly(4-methylstyrene) (P4MS), and poly(4-*tert*-butylstyrene) (PtBS)—was examined through dielectric relaxation (DR) measurements. Viscoelastic relaxation (VR) measurements were also conducted on the same samples to examine the segmental motion of polymer component.

The DR spectra of PS/5CB, P4MS/5CB, and PtBS/5CB mixtures reflecting the molecular motion of 5CB showed two relaxation processes (fast and slow modes). The slow mode was ascribed to the rotational motion of 5CB cooperative with the segmental motion of the polymers and the fast mode to the fluctuation motion of 5CB molecule in the confined space surrounded by less mobile polymer chains, respectively. The relative intensity of the fast mode increased with increasing the side chain bulkiness and/or the chain rigidity (represented by the Kuhn segment length). It was concluded that these two factors contribute to the increase of the relative amplitude of the fast mode relaxation.

The relaxation times of glass mode, τ_G, of three polymers were determined from the maximum frequency of the loss modulus spectra. Temperature dependence of τ_G was slightly different form that of τ_{slow}. From this difference in two relaxation times, we estimated the critical length of the rodlike molecule, L_c, with which the dielectric relaxation time of a rodlike molecule becomes equal to the viscoelastic relaxation time of the glass mode. The determined L_c values were comparable with the CRR (cooperative rearranging region) sizes reported so far, but no clear correlation was found between L_c and the Kuhn length. This result suggested that the length scale relevant to glassy dynamics was governed not only by the intramolecular segmental motion but also by the intermolecular cooperative motion.

The fast mode relaxation time, τ_{fast}, in the three mixtures decreased in the order of PS, P4MS, and PtBS, corresponding to the order of the side-chain bulkiness and main-chain stiffness, compared at a constant $T - T_g$. In contrast, the dielectric intensities of the fast mode increased in this order. From these results, it was concluded that confinement effect on

the fluctuation motion of a 5CB molecule became weaker in the order of PS, P4MS, and PtBS.

AUTHOR INFORMATION

Corresponding Author

*E-mail: nobukawa@jaist.ac.jp (S.N.); urakawa@chem.sci.osaka-u.ac.jp (O.U.).

Present Address

[§]Department of Environmental and Natural Resource Sciences, Tokyo University of Agriculture and Technology, Fuchu, Tokyo 183-8509, Japan.

Notes

The authors declare no competing financial interest.

ACKNOWLEDGMENTS

This work was partly supported by the Osaka University Global COE program, "Global Education and Research Center for Bio-Environmental Chemistry" from the Ministry of Education, Culture, Sports, Science, and Technology, Japan, by Grant-in-Aid for Scientific Research B and Research Activity Start-up from the Japan Society for the Promotion of Science (Grants 1806809, 20340112, 21350126 and 23850008) and by the Sasakawa Scientific Research Grant from the Japan Science Society (Grant 21-350).

REFERENCES

(1) Fox, T. G.; Flory, P. J. *J. Polym. Sci.* **1954**, *14*, 315−319.
(2) Adam, G.; Gibbs, J. H. *J. Chem. Phys.* **1965**, *43*, 139−146.
(3) Cangialosi, D.; Alegria, A.; Colmenero, J. *Phys. Rev. E* **2007**, *76*, 011514.
(4) Ferry, J. D. *Viscoelastic Properties of Polymers*, 3rd ed.; Wiley: New York, 1980.
(5) Williams, M. L.; Landel, R. F.; Ferry, J. D. *J. Am. Chem. Soc.* **1955**, *77*, 3701−3707.
(6) Angell, C. A. *J. Non-Cryst. Solids* **1991**, *131*, 13−31.
(7) Inoue, T.; Cicerone, M. T.; Ediger, M. D. *Macromolecules* **1995**, *28*, 3425−3433.
(8) Roland, C. M.; Ngai, K. L. *J. Non-Cryst. Solids* **1994**, *172*, 868−875.
(9) Kanaya, T.; Tsukushi, T.; Kaji, K.; Bartos, J.; Kristiak, J. *Phys. Rev. E* **1999**, *60*, 1906−1912.
(10) Hirose, Y.; Urakawa, O.; Adachi, K. *Macromolecules* **2003**, *36*, 3699−3708.
(11) Hirose, Y.; Urakawa, O.; Adachi, K. *J. Polym. Sci., Part B: Polym. Phys.* **2004**, *42*, 4084−4094.
(12) Ellison, C. J.; Mundra, M. K.; Torkelson, J. M. *Macromolecules* **2005**, *38*, 1767−1778.
(13) Urakawa, O.; Ohta, E.; Hori, H.; Adachi, K. *J. Polym. Sci., Part B: Polym. Phys.* **2006**, *44*, 967−974.
(14) Colmenero, J.; Arbe, A. *Soft Matter* **2007**, *3*, 1474−1485.
(15) Zheng, W.; Simon, S. L. *J. Polym. Sci., Part B: Polym. Phys.* **2008**, *46*, 418−430.
(16) Olson, B. G.; Srithawatpong, R.; Peng, Z. L.; McGervey, J. D.; Ishida, H.; Maier, T. M.; Halasa, A. F. *J. Phys.: Condens. Matter* **1998**, *10*, 10451−10459.
(17) Donth, E. *J. Non-Cryst. Solids* **1982**, *53*, 325−330.
(18) Capaccioli, S.; Ruocco, G.; Zamponi, F. *J. Phys. Chem. B* **2008**, *112*, 10652−10658.
(19) Fragiadakis, D.; Casalini, R.; Bogoslovov, R. B.; Robertson, C. G.; Roland, C. M. *Macromolecules* **2011**, *44*, 1149−1155.
(20) Runt, J. P.; Fitzgerald, J. J. *Dielectric Spectroscopy of Polymeric Materials*; American Chemical Society: Washington, DC, 1997.
(21) Yoshizaki, K.; Urakawa, O.; Adachi, K. *Macromolecules* **2003**, *36*, 2349−2354.
(22) Urakawa, O.; Nobukawa, S.; Shikata, T.; Inoue, T. *Nihon Reoroji Gakkaishi* **2010**, *38*, 41−46.
(23) Watanabe, H.; Urakawa, O. *Korea-Australia Rheol. J.* **2009**, *21*, 235−244.
(24) Colby, R. H. *Polymer* **1989**, *30*, 1275−1278.
(25) Miller, J. B.; McGrath, K. J.; Roland, C. M.; Trask, C. A.; Garroway, A. N. *Macromolecules* **1990**, *23*, 4543−4547.
(26) Adachi, K.; Fujihara, I.; Ishida, Y. *J. Polym. Sci., Part B: Polym. Phys.* **1975**, *13*, 2155−2171.
(27) Taniguchi, N.; Urakawa, O.; Adachi, K. *Macromolecules* **2004**, *37*, 7832−7838.
(28) Ediger, M. D.; Inoue, T.; Cicerone, M. T.; Blackburn, F. R. *Macromol. Symp.* **1996**, *101*, 139−146.
(29) van den Berg, O.; Wubbenhorst, M.; Picken, S. J.; Jager, W. F. *J. Non-Cryst. Solids* **2005**, *351*, 2694−2702.
(30) Inoue, T. *Macromolecules* **2006**, *39*, 4615−4618.
(31) Matsumiya, Y.; Uno, A.; Watanabe, H.; Inoue, T.; Urakawa, O. *Macromolecules* **2011**, *44*, 4355−4365.
(32) Nobukawa, S.; Urakawa, O.; Shikata, T.; Inoue, T. *Macromolecules* **2011**, *44*, 8324−8332.
(33) McLeish, T. C. B. *Adv. Phys.* **2002**, *51*, 1379−1527.
(34) Rouse, P. E. *J. Chem. Phys.* **1953**, *21*, 1272−1280.
(35) Erwin, B. M.; Masser, K. A.; Colby, R. H. *J. Non-Cryst. Solids* **2006**, *352*, 4776−4784.
(36) Ding, Y.; Sokolov, A. P. *J. Polym. Sci., Part B: Polym. Phys.* **2004**, *42*, 3505−3511.
(37) Maconnachie, A.; Fried, J. R.; Tomlins, P. E. *Macromolecules* **1989**, *22*, 4606−4615.
(38) Fetters, L. J.; Lohse, D. J.; Milner, S. T.; Graessley, W. W. *Macromolecules* **1999**, *32*, 6847−6851.
(39) Inoue, T.; Matsui, H.; Osaki, K. *Rheol. Acta* **1997**, *36*, 239−244.
(40) Fetters, L. J.; Lohse, D. J.; Richter, D.; Witten, T. A.; Zirkel, A. *Macromolecules* **1994**, *27*, 4639−4647.
(41) Debye, P.; Ramm, W. *Ann. Phys. (Berlin, Ger.)* **1937**, *28*, 0028−0034.
(42) Kirkwood, L. G. *J. Chem. Phys.* **1939**, *7*, 911.
(43) Onsager, L. *J. Am. Chem. Soc.* **1936**, *58*, 1486−1493.
(44) Havriliak., S.; Negami, S. *Polymer* **1967**, *8*, 161−210.
(45) Cole, K. S.; Cole, R. H. *J. Chem. Phys.* **1941**, *9*, 341−351.
(46) Roland, C. M.; Ngai, K. L.; Plazek, D. J. *Macromolecules* **2004**, *37*, 7051−7055.
(47) Inoue, T.; Onogi, T.; Yao, M. L.; Osaki, K. *J. Polym. Sci., Part B: Polym. Phys.* **1999**, *37*, 389−397.
(48) Doi, M.; Edwards, S. F. *The Theory of Polymer Dynamics*; Oxford University Press: New York, 1986.
(49) Colby, R. H. *Phys. Rev. E* **2000**, *61*, 1783−1792.
(50) Erwin, B. M.; Colby, R. H. *J. Non-Cryst. Solids* **2002**, *307*, 225−231.
(51) Donth, E. *Acta Polym.* **1984**, *35*, 120−123.
(52) Williams, G.; Watts, D. C. *Trans. Faraday Soc.* **1970**, *66*, 80−85.
(53) Koizumi, N.; Kita, Y. *Bull. Inst. Chem. Res., Kyoto Univ.* **1978**, *56*, 300−339.
(54) Li, H. L.; Ujihira, Y.; Nanasawa, A. *J. Radioanal. Nucl. Chem.* **1996**, *210*, 533−541.
(55) Bergman, R.; Alvarez, F.; Alegria, A.; Colmenero, J. *J. Chem. Phys.* **1998**, *109*, 7546−7555.